PII: S0955-2219(98)00139-3

0955-2219/98/$—see front matter

Interaction of Barium Titanate Powders with an Aqueous Suspending Medium

M. C. Blanco López,* G. Fourlaris and F. L. Riley

Department of Materials, University of Leeds, Leeds LS2 9JT, UK

(Received 31 March 1998; accepted 16 June 1998)

Abstract

Characterisation by SEM, TEM and XPS of $BaTiO_3$ powders that have been exposed to water provides an assessment of the extension of their interaction with the suspending medium. Ba^{2+} ions are released into the aqueous solution when powder suspensions are prepared, as detected by atomic absorption spectroscopy, but it appears that their presence in the aqueous medium is due to dissolution of $BaCO_3$ present in the powders as an impurity. No changes in morphology of the powders or composition of the surface were observed, a part from precipitation of $BaCl_2$ on the surface of the particles when the pH was lowered with HCl. However, a ~20 nm layer depleted in Ba^{2+} develops at the surface of undoped sintered materials after exposure to water, as a result of the partial hydrolysis of the $BaTiO_3$, which affect in less extent to Nb-doped sintered material.

1 Introduction

Organic solvents such as ethanol or trichloroethene (or azeotropic mixtures of both) have been used for many years as dispersing media for the preparation of $BaTiO_3$ tape-casting slurries. For safety, environmental and economic reasons, there is a need to move away from the use of organic liquids towards water. The first step in the study of the aqueous $BaTiO_3$ dispersion is the evaluation of the interaction of the powder with the suspending medium, which has to meet critical requirements, such as being a good solvent for the dispersants, binders and plasticisers, and having minimal reaction with the powder.[1]

*To whom correspondence should be addressed. Present address: Instituto Nacional del Carbón, La Corredoria, Apartado 73, 33080 Oviedo, Spain. E-mail: mcblanco@muniellos.incar.csic.es

Partial solution is potentially an important problem in the aqueous phase processing of $BaTiO_3$ powders in particular, because of the changes caused in the stoichiometry of the particle surface and a redistribution of the components within the final powder. The presence of a liquid phase on the TiO_2-rich side of the phase diagram at temperatures in the region of 1300–1350°C[2] will enhance the tendency for the exaggerated grain growth. This is an undesirable effect in electronic devices, since it is well known that the dielectric constant of barium titanate ceramics decreases with increasing grain size.[3,4] Exaggerated grain growth in $BaTiO_3$ ceramics has been seen as a result of milling the powder in water.[5] High concentration of barium ions are present in solution after milling of $BaTiO_3$ powders water[5] and polar organic media (formamide and *n*-methyl formamide) with similar properties to water such as high dielectric constant and good ionic solvation capacity.[6] These observations have been taken as evidence for the selective dissolution of BaO from $BaTiO_3$.

On the other hand, titanates have generally been regarded as insoluble in water: this has been one of the reasons for their inclusion in the formulation of synthetic rocks ('Synroc') for the storage of high activity nuclear waste materials. In this context, the stability of titanate minerals with the $CaTiO_3$ perovskite structure has been studied under high temperature and pressure[7,8] (hydrothermal conditions).

The hydrolysis reaction can be regarded as follows:

$$BaTiO_{3(s)} + H_2O_{(1)} = Ba^{2+}_{(aq)} + TiO_{2(rutile)} + OH^-_{(aq)} \quad (1)$$

Moreover, in laboratory and industrial normal environments the situation is in reality more complicated because of the presence of dissolved carbon dioxide. A second equilibrium:

$$BaTiO_{3(s)} + CO_{2(soln.)} = BaCO_{3(s)} + TiO_{2(rutile)} \quad (2)$$

has to be taken into account. This has the effect of increasing $BaTiO_3$ solubility through the solubility of $BaCO_3$ unless pCO_2 (and thus the concentration of CO_2 in solution) is extremely low.

$$BaCO_{3(s)} + H_2O_{(1)} = Ba^{2+}_{(s)} + HCO_3^-(s) + OH^-_{(s)} \quad (3)$$

Lencka and Riman[9] have proved the necessity for thermodynamic modelling of the ceramic powder system to identify the best conditions for the synthesis, and the hydrothermal synthesis of $BaTiO_3$ was used as an example of this procedure, together with other perovskites with electronic applications such as $PbTiO_3$ and $SrTiO_3$.[9,10] Several stability diagrams were produced for $BaTiO_3$ in aqueous environment, as a function of pH and Ba^{2+} concentration. They showed that $BaTiO_3$ was only thermodynamically stable in water at high pH and high Ba^{2+} ion concentration. This approach was later applied to the production of $BaTiO_3$ films.[11] Other phase diagrams for the Ba–Ti–H_2O system and Ba–Ti–CO_2–H_2O systems have been reported[12,13] for the ideal conditions (when activities can be approximated to concentrations). However, the method followed by Lencka and Riman is more strict and includes the calculation of activity coefficients and a comparison of the effects of different sources of thermodynamic data. It has to be noted, however, that for the reverse process (dissolution of $BaTiO_3$, not synthesis), these equilibria may be in practice very slow to be attained at room temperature and that the rate of dissolution is likely to depend on solid state diffusion processes occurring in the subsurface regions of the barium titanate particle.

With the aim of evaluating the kinetic aspects of $BaTiO_3$ and other related titanates hydrolysis, leaching rates for the partial dissolution at different temperatures, obtained with sintered discs on the basis of ion concentration in solution, and averaged over different periods of time, have been reported (Table 1).[7,14] Leaching rates measured with $BaTiO_3$ powders might not be completely reliable because of the possibility of contamination by $BaCO_3$[15]: the solution rates measured could be those of the more soluble carbonate. The rates for $SrTiO_3$ and $BaTiO_3$ are very similar, and one to two orders of magnitude higher than those for $CaTiO_3$. The values appear to be lower at higher temperatures, because precipitation of the alkaline earth oxides was observed under those conditions.[14]

Table 1. Leaching rates for titanates at various temperatures ($\mu g\ m^{-2}\ s^{-1}$) over 7 days, (1) from Ref. 7; (2) from Ref. 14

	$25°C^{(1)}$	$100°C^{(1)}$	$200°C^{(1)}$	$300°C^{(1)}$	$300°C^{(2)}$
$CaTiO_3$	< 1·1	0·1	—	0·1	0·16
$SrTiO_3$	2·3	3·7	0·70	0·5	—
$BaTiO_3$	1·1	4·0	0·92	0·35	0·382

The results reported for dissolution of $CaTiO_3$ are relevant to this study, since both $CaTiO_3$ and $BaTiO_3$ have the perovskite structure. By monitoring the changes in chemical composition of the species present at the surface after consecutive bombardment with Ar^+ ions, a layer depleted in Ca was found for $CaTiO_3$ discs after 19 days at 300°C.[16] A depleted layer 200 nm thick was also found after leaching $BaTiO_3$ at 250°C for 12 days.[14] A ~8 nm layer was identified by TEM showing a Ti–O amorphous layer on the edges of a perovskite surface ion beam thinned specimen (1 day at 110°C and 180 kPa in distilled water).[17]

Even at room temperature, it has been found that $CaTiO_3$ samples in contact with water developed a similar 10 nm amorphous layer within the first 9 h.[18] At 60°C the thickness of this layer increased to 20 nm, and the rate for the release of Ca^{2+} ions was higher. This surface layer was identified only with single crystal particles in contact with low concentrations of Ca^{2+} ($< 10^{-5}$ mol dm^{-3}) at pH 9·5. In the case of polycrystalline materials, a similar layer was found only on the fragments that had been removed from an attacked and cut surface. The hydroxide species $Ca(OH)^+$ or $Ca(OH)_2$ were detected by surface analytical techniques on the $CaTiO_3$ surface.[18] The low binding energy hydroxide and carbonate were detected by XPS.[14] On this basis, a dissolution mechanism for $CaTiO_3$ single crystal was formulated[18] in which $CaTiO_3$ is considered to be a Ti–O lattice with Ca^{2+} ions occupying the octahedral sites; the dissolution starts by an interchange procedure between H^+ ions in the H_2O and Ca^{2+} at the surface, provided that the Ca^{2+} concentration in solution is less than 10^{-5} mol dm^{-3}. This mechanism appeared to be catalysed by OH^- ions. Dissolution progresses, developing a Ti–O ($Ti(OH)_x$) layer at the surface, until this layer is thick enough to severely retard the outwards diffusion and release of the more inner Ca^{2+} ions. This hydroxyl layer can also incorporate species such as $Ca(OH)^+$ and $Ca(OH)_2$.

The mechanism suggested for the dissolution of these and similar titanates under hydrothermal attack is very similar.[14,16] The main difference reported between hydrothermal and room temperature attack is that recrystallised TiO_2 phases

(brookite and rutile) are only found at temperatures above 120°C.[18]

This study reports on the characterisation of $BaTiO_3$ powders (which have either been exposed to water or acid-washed) through the use of scanning and transmission electron microscopy (SEM and TEM) and X-ray photoelectron spectroscopy (XPS) for surface analysis. The concentration of Ba^{2+} ions released was measured by atomic absorption. Disc specimens were used for depth profiling of a $BaTiO_3$ surface exposed to water. The data reported here provide the basis for important conclusions relevant to the dispersion of $BaTiO_3$ powder in aqueous media and the preparation of aqueous tape casting suspensions.

2 Experimental

2.1 Materials

The $BaTiO_3$ powders used in this study are listed in Table 1. More detail about the characteristics of these powders can be found in Ref. 15. A1 and A2 were two different supplies of the same batch of a Nb-doped powder. Powder B had an average particle size of $\sim 0{\cdot}5\,\mu$m, and A1, A2 and C$\sim 1{\cdot}5\,\mu$m. A1, A2 and C were made by solid state route reaction between $BaCO_3$ and TiO_2; B was an undoped powder, made by an oxalate route. The range of estimated $BaCO_3$ contamination in these powders[15] is shown also in Table 2.

2.2 Methods of examination

2.2.1 Atomic absorption (AA)

One gram of powder was allowed to stand during 48 h in 30 cm^{-3} of deionised H_2O at different pHs (adjusted with HCl or KOH) in a normal atmosphere. The suspensions were then centrifuged and the liquid supernatant collected for atomic absorption analysis, (Varian SpectrAA-10) of barium and titanium calibrated with standard solutions. One set of dispersions of powder A1 were prepared in freshly boiled water and kept under N_2 flowing atmosphere, in order to observe any possible difference between the CO_2 free and the normal atmosphere conditions.

2.2.2 TEM examination

For the TEM study a Philips EM 430 HVEM operating at an accelerating voltage of 300 KV fitted with a Line ISIS EDS-system was used. A small amount of powder A1 was dispersed by ultrasonic probing in isopropanol (the reference powder), and in water at pH 9 (the end point) and 4 (maintained with HCl additions), and allowed to stand for 2 days. After sedimentation, a few drops of the supernatant were taken and deposited on a copper grid coated with a carbon film. Additional samples were prepared leaving some powder unstirred in a hydrochloric acid solution at pH 4 for 12 h. The aqueous suspensions were then centrifuged and decanted. The powder was washed with isopropanol twice, which was evaporated at low temperature, and redispersed in the same solvent for TEM examination.

For selected area diffraction patterns (SADP) the selected aperture was 500 μm. The EDS beam probe size was 30–50 nm.

2.2.3 SEM study

A CamScan series 4 SEM (Cambridge Instruments, Cambridge, UK) was used, fitted with a EDS system (Link 860 system analyser). As for the TEM study, the powder examined was dispersed in isopropanol, and in water at pH 9 and 4. A few drops of the suspension in every case were taken, and allowed to dry on an aluminium stub covered with a thin polished glass cover slip. The powder film was then gold coated.

2.2.4 Surface analysis XPS

Powder specimens were prepared using an aluminium stub with commercial double sided adhesive tape on which the powder sample adhered. Two sets of samples were prepared with powders A1 and B: as received, and powder left unstirred in aqueous hydrochloric acid solution for 12 h, washed later in isopropanol and dried, as described in Section 2.2.2.

In order to assess quantitatively the extent of interactions between $BaTiO_3$ materials and water with depth, 3 disks 1 cm diameter were made with powders A1 and B by die pressing and sintering in air at 1360°C for 2 h to a density of ~94% of theoretical. They were then polished with diamond paste to 3 μm. This procedure is very similar to the one reported earlier.[19,20] Since interaction with water was being assessed, all contact with water was carefully avoided during the initial preparation and polishing steps. One disc was immersed in deionised water (pH~6) for 24 h, a second was immersed in pH 3 for 24 h, and a third disc was left untreated, as a reference. The surfaces were rinsed with methanol and allowed to dry.

XPS spectra were recorded with a Kratos XSAM 800 spectrometer using Mg K_α (1253·6 eV) excitation. Ion etching was performed by 2·5 KeV Ar^+ ions (Kratos MacroBeam ion gun) with $3{\cdot}4\times10^{-6}$ A cm^{-2} current density. The sputter rate was ~1 nm/min. Data acquisition and processing, including quantification, were performed with the Kratos Vision 2000 software. Only the most sensitive peaks for each surface element were analysed

(i.e. C 1s, O 1s, Ti 2p 3/2 and Ba 3d 5/2) using powders and sintered discs. The assignation of chemical states was made when possible with literature binding energy values.[21,22]

3 Results

3.1 Atomic absorption analysis

Ba^{2+} ions were released from all the powders when they were stirred with water at room temperature under normal laboratory air environment and also under CO_2 free atmosphere. The initial release of Ba^{2+} was reported to be very fast in an earlier study, and appeared to reach a plateau (equilibrium) after approximately 6 h.[23] The steady state Ba^{2+} concentration in solution was measured after 24 h, as a function of pH (Fig. 1). A maximum value of $\sim$200 mg dm^{-3} was reached with powders A_1 and A_2 at pH 2, $\sim$450 mg dm^{-3} with powder B and $\sim$800 mg dm^{-3} with powder C at pH 3. The Ba^{2+} released increased most markedly for pH values below 7. Titanium ions could not be detected by atomic absorption, and the Ti concentration must therefore have been < 1 mg dm^{-3} (the limit of detection of the instrument used).

The key question was now the extent to which these ions were released by dissolution of the $BaTiO_3$ particle surface according to reaction (1) or from solution of the free $BaCO_3$ previously identified[15] [Reaction (3)]. This was addressed using the following range of experimental techniques.

3.2 Electron microscopy

Powder dispersed in water at pH 4 and 9 was examined by TEM to try to detect any change in structure which might have taken place at the particle surfaces. Several EDS-X ray microanalysis and selected area diffraction patterns (SADP) were recorded for the powder in the reference condition (as received and dispersed in IPA), and showed that the powder was tetragonal $BaTiO_3$ (Fig. 2),

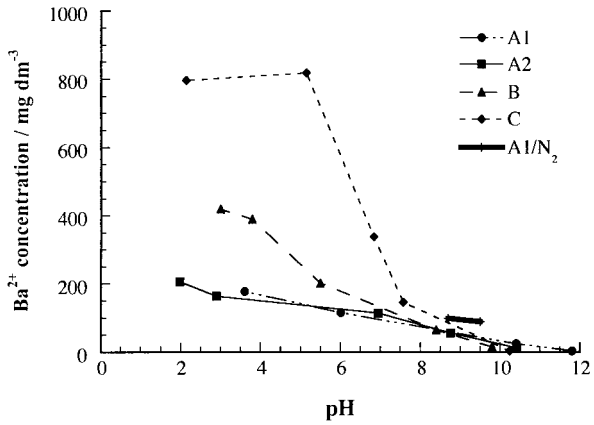

Fig. 1. Ba^{2+} concentration measured in solution after 48 h.

and the samples prepared this way were therefore representative of the batch, which was found to correspond to tetragonal $BaTiO_3$.[15] Only tetragonal $BaTiO_3$ was identified with conventional transmission microscopy techniques, in the sample suspended at pH 9 (Fig. 3). Since most of the particles appeared relatively thick under the electron beam of the TEM, lattice imaging was not carried out. When the powder which had been suspended at pH 4 was examined, Cl (in addition to Ba, Ti and O) was identified by EDS-X-ray microanalysis on the majority of the examined particles (Fig. 4). Morphological studies using bright field micrographs in Fig. 4 showed the presence of deposition products on the $BaTiO_3$ particles, altering the smooth surface appearance of the particles (compare with Fig. 3), to the mottled effects observed in Fig. 4. Selected area diffraction pattern (SADP) analysis revealed that this surface product was cubic $BaCl_2$

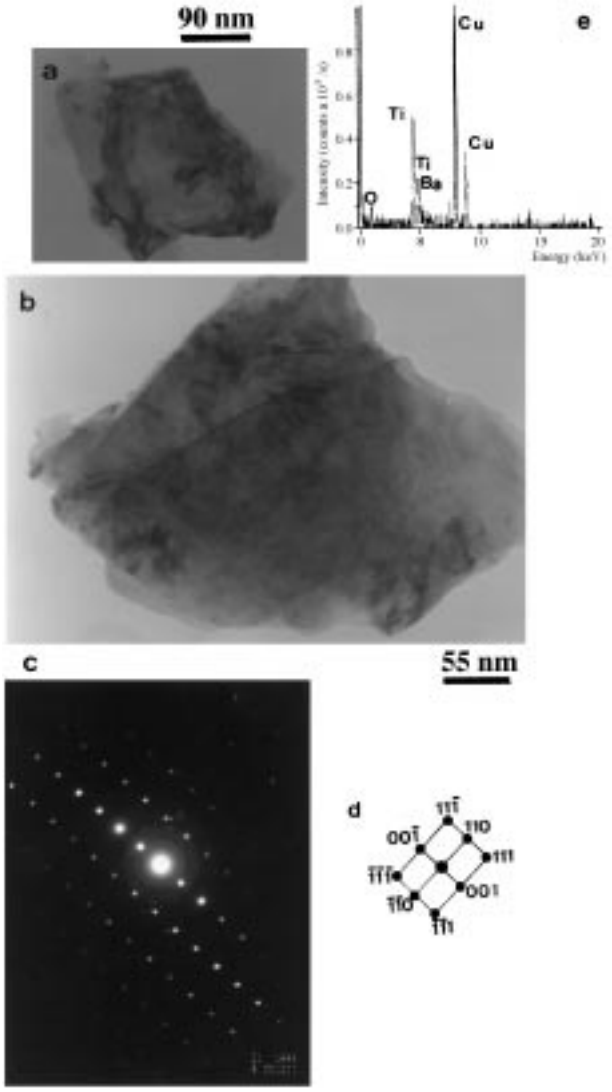

Fig. 2. (a) Bright field TEM micrograph of a $BaTiO_3$ particle (powder A1) suspended in IPA; (b) bright field TEM micrograph of the same particle at higher magnification; (c) SADP of the particle in (a) and (b); (d) indexing of the SADP; (e) EDS-D-ray spot microanalysis spectrum of the particle in (a).

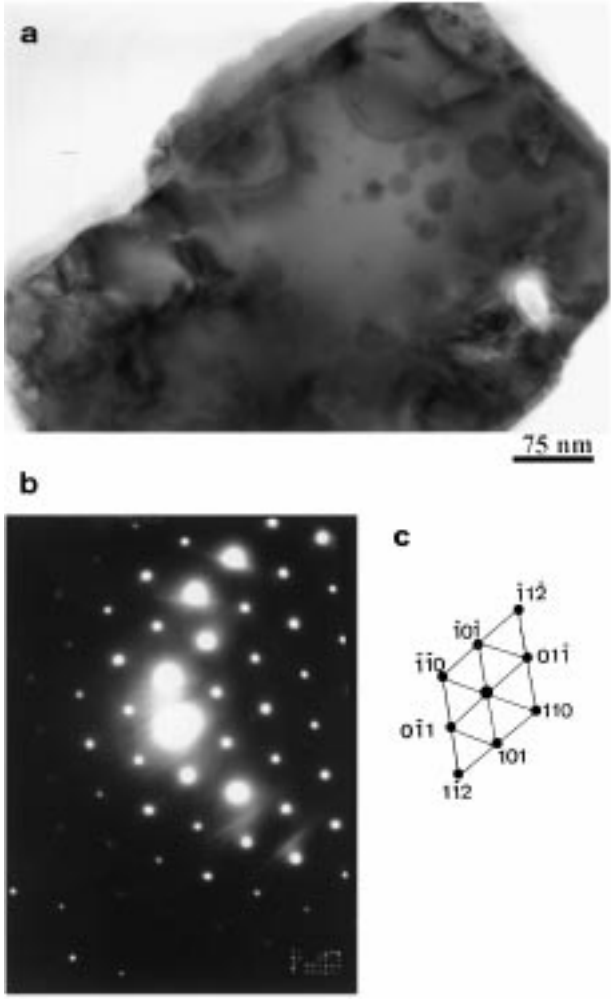

Fig. 3. (a) Bright field TEM micrograph of a tetragonal $BaTiO_3$ particle (powder A1) suspended in H_2O at pH 9; (b) SADP of the particle in (a); (c) indexing of the SADP.

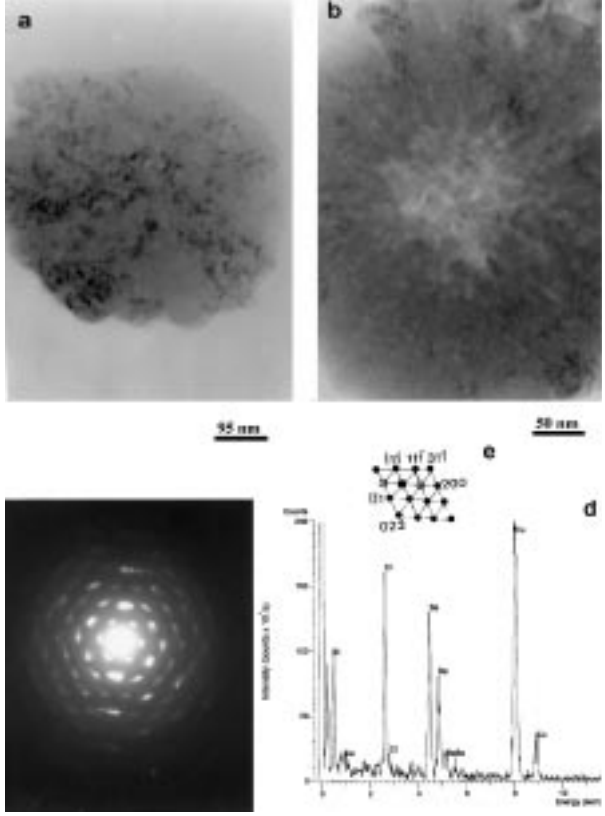

Fig. 4. (a) Bright field TEM micrograph of a $BaTiO_3$ particle (powder A1) suspended in H_2O at pH 4; (b) higher magnification TEM micrograph of the same particle; (c) SADP of the particle in (a); (d) EDS-X-ray spectrum of the centre of the particle in (a); (e) indexing of the SADP.

[Fig. 4(c)]. No other surface film or product was identified on the $BaTiO_3$ particles. A study of powder that had been washed at pH 4 and redispersed in IPA did not show the presence of any amorphous layer on the surface.

Shape and morphology of the powders did not change as observed by SEM after exposure to water and acid wash.

3.3 XPS analysis of the powder particle surface and polycrystalline discs of $BaTiO_3$

The surface of both powders was analysed as-received and after an acid wash. Four elements were found in both powders: C, O, Ba and Ti. The transitions analysed were the most sensitive ones for each element, i.e. C 1s, O 1s, Ba 3d5/2, and Ti 2p3/2. These results are shown in Tables 2–4. A correction for the C, identified as hydrocarbon contamination from the ultra high vacuum chamber has been made, in order to better compare the stoichiometry of the other components of the surface. Atomic concentrations were converted to atom ratio with the same purpose.

Table 5 shows that the Ti/Ba ratios found on the surface of the powders by XPS is higher than the Ti/Ba ratio found by the XRF analysis of the powders, and that these ratio increase after the acid wash.

The same chemical elements were found on the surface of all the sintered disks (treated and untreated) of powder A1 and B analysed. The only differences as compared with the analysis of the particles surface are that, in this case, more than one chemical state for carbon was clearly identified

Table 2. $BaTiO_3$ powders used in this study

Powders	*Producers*	*Characteristics*	*Estimated $BaCO_3$ content (wt%)*[15]
A1	Lot 219-3 Transelco Ferro New York, USA	Nb-doped	0·6
A2	Lot 219-3 Transelco Ferro New York, USA	Nb-doped	0·9
B	HPB-MBB lot 10 Tam Ceramics Niagara Falls, USA	Undoped	1·8
C	Lot 427 Cookson Ceramics, Wallsend, UK	Undoped	3·5

Table 3. XPS results for A_1

Element	Centre (eV)	A1 as received		A1 after acid wash	
		Atomic Conc. (%)	Atomic ratio (Corrected for C vac. cont.)	Atomic Conc. (%)	Atomic ratio (Corrected for C vac. cont.)
C ls	284·6	23·0	—	7·4	—
Ti 2p3/2	458·2	15·5	1·0	21·1	1·0
1 O 1s	529·5	40·5	2·6	48·5	2·3
2 O ls	531·4	13·2	0·8	14·3	0·7
1 Ba 3d5/2	778·9	5·7	0·4	6·1	0·3
2 Ba 3d5/2	780·6	2·1	0·2	2·7	0·1

Table 4. XPS results for powder B

Element	Centre (eV)	B as received		B after acid wash	
		Atomic Conc. (%)	Atomic ratio (Corrected for C vac. cont.)	Atomic Conc. (%)	Atomic ratio (Corrected for C vac. cont.)
C ls	284·6	25·7	—	27·6	—
Ti 2p3/2	458·2	11·7	1·0	12·0	1·0
1 O 1s	529·5	36·0	3·1	32·1	2·7
2 O ls	531·4	19·0	1·6	22·2	1·8
1 Ba 3d5/2	778·9	5·4	0·5	4·4	0·4
2 Ba 3d5/2	780·6	2·1	0·2	1·8	0·2

for both discs at 286·1 and at 288·4 eV, and a third component in the O1s envelope at 532·9 eV has also been found. The lower BE component of Ba 3d5/2 (at 779·0 eV) and the higher BE components of O1s together with C at 288·4 eV, disappear after the first 2 min of Ar^+ bombardment (2 nm). By comparison with the BE values reported for $BaCO_3$, this can be interpreted as the presence of a $BaCO_3$ layer, 2 nm thick at the surface of the disks. Only the Ba component at 780·1 and O1s at 529·3 eV (assigned to $BaTiO_3$) remain with depth.

The only changes in BE after the removal of the first 2 nm of surface was the development of shoulders on the Ti envelope at BE values ~458 eV. This is the result of the reduction of Ti^{4+} to Ti^{3+}, a well-established phenomenon in titanates.[24–26] After the loss of the first ~2 nm of material, no preferential sputtering of Ba or O from the sintered discs was detected, as indicated by the constant O/Ba and Ba/Ti ratios with sputtering time, shown in Fig. 5. After washing in water at pH 3 the sintered Nd-doped powder A1 showed a weak release of Ba^{2+}, most of which took place from the first 20 nm (Fig. 6). Within experimental error of the measurements, there was no difference in behaviour between an untreated surface and a surface washed in water at pH 6. In contrast the sintered undoped powder B released Ba to a depth of ~30 nm after 24 h exposure to acidic conditions, with a marked loss over the first 10 nm. In this case there was no clear difference for pH 3 and pH 6 (Fig. 7).

Table 5. Ti/Ba ratio of the $BaTiO_3$ powders. Comparison between surface analysis by XPS and bulk analysis by XRF

Powder	Ti/Ba ratio by XRF	Ti/Ba ratio by XPS before acid wash	Ti/Ba ratio by XPS after acid wash
A1	1·06	1·7	2·5
B	1·06	1·4	1·7

4 Discussion

The primary objective of this examination of $BaTiO_3$ powders was to assess the extent to which surface reactions occurred on exposure to water. A recognised complication with this system was the presence of ~1 to ~3% $BaCO_3$ as a second phase contaminant. There were thus two potential origins of the Ba^{2+} released to the aqueous phase: the $BaTiO_3$ surface, and the $BaCO_3$, most probably present as a second particulate phase, rather than a particle coating.[15] The release of Ba^{2+} from the $BaCO_3$ was moreover potentially able to influence equilibrium relationships at the $BaTiO_3$ surfaces. In order to assess semiquantitatively the possible leaching of ions from the $BaTiO_3$ it was necessary to use sintered discs, because of the difficulties of interpretation of the depth profiles obtained on powder samples.

4.1 Powders

Ba^{2+} ions are released into solution from both $BaTiO_3$ powder suspensions. The equilibrium concentration increased from ~0 at pH 12 to ~200 mg dm^{-3} for A_1 and A_2, 450 for B, and ~800 mg dm^{-3} for powder C (Fig. 1). In this experiment, powders

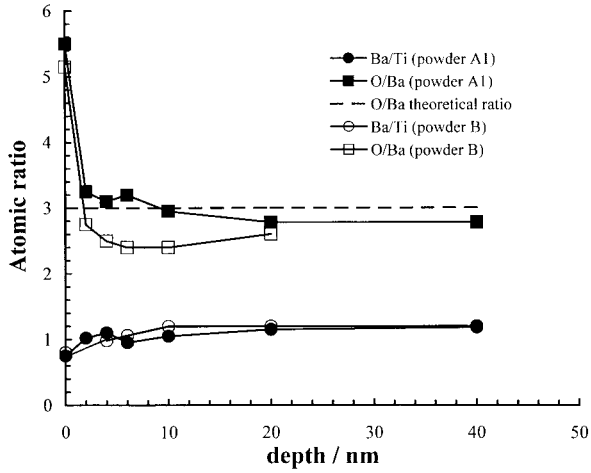

Fig. 5. Effect of Ar^+ bombardment on the Ba/Ti and Ba/O ratios at the surface of untreated sintered discs of $BaTiO_3$.

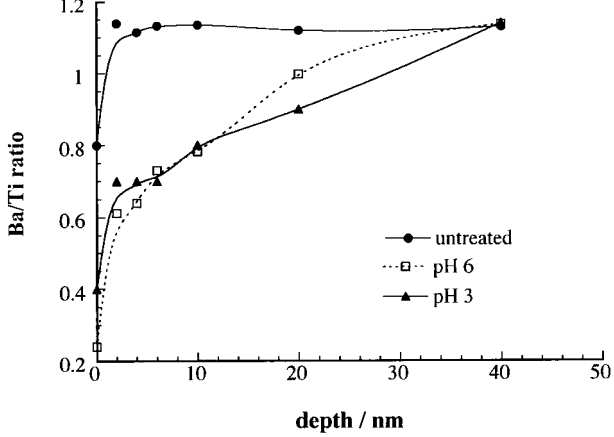

Fig. 6. Effect of the aqueous treatment (24 h in deionised water at pH 6 and 3) on the Ba/Ti ratio at the surface of a sintered disc of powder B.

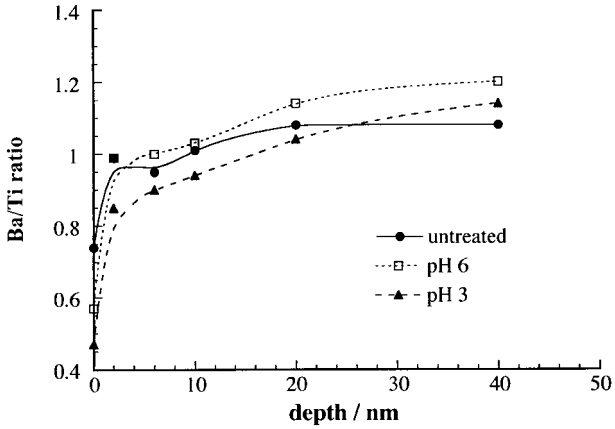

Fig. 7. Effect of the aqueous treatment (24 h in deionised water at pH6 and 3) on the Ba/Ti ratio at the surface of a sintered disc of powder A1.

were allowed to remain unstirred in the suspension. A similar relationship between concentration and pH has been determined for $BaTiO_3$ powders milled in water,[5] in this instance a much higher range of concentrations was measured (1000–6000 mg dm^{-3}), and this is likely to be related to the readier release of barium ions from freshly fractured and higher energy $BaTiO_3$ surfaces. However, there is no evidence that the source of these Ba^{2+} ions is the $BaTiO_3$ itself.

Table 6. XPS results for the analysis of the surface of sintered discs of $BaTiO_3$ powder (A1: Nb-doped; B: undoped)

Element	*Centre (eV)*	*Untreated A1 Atomic conc (%)*	*Untreated B Atomic conc (%)*
1C 1s	285·0	32·2	36·9
2C 1s	286·2	7·5	5·0
3C 1s	288·7	2·9	3·7
Ti 2p 3/2	458·2	9·8	9·3
1O 1s	529·8	24·4	22·0
2O 2s	531·5	11·9	12·2
3O 3s	532·9	3·4	3·5
1 Ba 3d 5/2	779·2	4·2	4·0
2 Ba 3d 5/2	780·5	3·7	3·3

When the experiment was carried out under flowing N_2 (CO_2 free atmosphere), the concentrations of Ba^{2+} measured were slightly higher. Solubility of $BaTiO_3$ should be lower under this conditions, and the only explanation for this finding is that bubbling N_2 through the dispersion had the effect to better disperse the powder and facilitate this way the dissolution of the $BaCO_3$ present.

If $BaTiO_3$ particles undergo dissolution, an amorphous layer at the surface, in which the Ba^{2+} concentration is depleted could be expected. However, no amorphous layer was observed by TEM on the surface of the particles, neither the morphology of the particles changed after an acid wash, as observed under SEM. It is possible that the amorphous layer observed in Ref. 18 at the surface of particles collected after cutting $CaTiO_3$ specimens and immersed in water is due to acceleration of the hydrolysis reaction by the high temperatures and pressures reached during the cutting process.

Two different chemical states were found for Ba and O on the surface of the powders (Tables 3 and 4), in agreement with previous reported results.[15,27,28] This appears to be a common feature of the $BaTiO_3$ particle surface, related to crystalline distortions. Further experiments are necessary to confirm this hypothesis, but what is important at this stage is that there is not evidence for a $BaCO_3$ film, since there is no a high BE component (at ~288·5 eV) for C. This point has been discussed in detail in Ref. 15. The only C state identified was the unavoidable contamination with hydrocarbon in the ultra high vacuum chamber. The most relevant conclusion from this XPS analysis in this study is that none of the Ba components decreased significantly after an acid wash, as it would have been expected if dissolution occurred (Tables 3 and 4).

$BaCO_3$ is normally considered to be partly soluble in water (the solubility in water at 25°C is reported to be ~23 mg dm^{-3}) and totally soluble in acidic pH.[29] With adjustment of the pH to lower values by the addition of small amounts of (hydrochloric) acid, $BaCO_3$ becomes completely soluble:

$$CO_3^{2-}(aq) + 2H^+(aq)2 = CO_2(g) + H_2O \qquad (4)$$

The Ba^{2+} concentrations found in solution at acidic pH (2–4) correspond to the levels of $BaCO_3$ contaminant present in the $BaTiO_3$ powders (Table 1), confirming that they are originated by dissolution of the $BaCO_3$, and not $BaTiO_3$. The Ba^{2+} (aq) ions will recombine on drying to redeposit thin films of barium chloride (after loss of

CO_2) on the particles surfaces, as observed by TEM (Fig. 4). This suggests that these low pH values should be better avoided during the preparation of aqueous suspensions for tape casting. The hydrolysis of $BaCO_3$ might suppress any dissolution of the $BaTiO_3$, because the concentration of Ba^{2+} in solution is already high.

4.2 Dissolution from sintered polycrystalline $BaTiO_3$

Sintered discs were used for compositional profiles because of the necessity for a flat surface. Care is, however, needed in extrapolating data obtained on polycrystalline material to powder particle surfaces because of possible effects related to the presence of the grain boundaries. Within the boundaries the energies and therefore mobilities of ions are likely to be different from those of ions in the bulk of the crystal lattice. Equally, the energies and mobilities of ions in bulk single crystal are likely to be different from those in very small particles, because of surface energy compression of the lattice.

Surface analyses on the sintered material and ground surfaces showed three chemical states for C1s. The peak at 284·6 eV is associated with the normal hydrocarbon contamination; the other two peaks are associated with forms of C–O bonding. The weak peak at 286·2 eV is considered to be that of the simple C–O group; this could correspond to residual methanol used to rinse the surface. The peak at 288·7 eV has been identified with the carbonate CO_3^{2-} environment (chemisorbed CO_2). Of the three oxygen peaks, that at 531 eV is also associated with a simple C–O bond, and that at 531·5 eV with the carbonate group. So there is clear and strong evidence for the presence at the disc surfaces of barium carbonate.

A single state for Ti was identified, at the BE corresponding to $BaTiO_3$ (458·2 eV). Three states for O, that at 532·8 eV related to the C–O bond, that at 531·4 eV related to the carbonate group, and that at 529·6 eV to $BaTiO_3$. The same states for Ba were found on the surface of the discs and the surface of particles, at 779·0 and 780·5, separated by the same BE (1·5 eV). On the basis of the existence of C as carbonate and the literature values for Ba in $BaCO_3$, we can assume that the higher BE component at 780·5 eV is associated to $BaCO_3$ in this case. There were no significant differences in peak position or relative intensity, between the discs prepared from the A1 and B powders.

The detection of adsorbed CO_2 on the surfaces of the sintered material, and which was not seen on the surfaces of particles of the corresponding powders, may be explained in terms of the CO_2–$BaTiO_3$ domain dipole–dipole interaction.[30] This interaction, providing a driving force for the strong adsorption of CO_2 at a $BaTiO_3$ surface, is available for the polycrystalline $BaTiO_3$, but not for the $\sim 1\,\mu m$ $BaTiO_3$ powder used here, for which the ferroelectricity would be very weak. The existence of the second (carbonate) carbon is in consequence readily explicable in terms of the tendency for physisorbed CO_2 in the titanate surface O^{2-} ions, to rearrange and convert to chemisorption and the development of CO_3^{2-} groups.[31,32] The 779·0 eV (non-perovskite) Ba(1) peak disappears after the first few minutes of argon ion bombardment, indicating that it is in the first monolayers of the surface. It is also assigned therefore to the chemisorbed CO_2 layer.

The conclusion drawn from these examinations of the untreated and treated ground surfaces is that the outer layer to a depth of around 2 nm contains a high concentration of the CO_3^{2-} group, corresponding to the presence, in effect of a 'barium carbonate' surface film, which formation has been reported to be time dependent.[33]

There are contradictory reports about the preferential sputtering of titanates under argon ion bombardment. It has been reported that titanates decompose loosing preferentially O and Ba;[34–36] however, this effect was not detected during depth profiling examination of $BaTiO_3$ single crystal by Auger electron spectrometry.[37] Preferential sputtering would clearly have been a significant block to the detection of any changes in Ba/Ti ratio with depth, resulting from a selective release of Ba^{2+} into the aqueous phase. The present XPS examinations appear to have confirmed the absence of preferential sputtering (Fig. 5).

Exposure to water at pH 3 results in changes to the surface layer in both types of material, but the changes are much more pronounced and penetrate to a greater depth ($\sim$25 nm) for material prepared from the undoped $BaTiO_3$ (B) powder. The Nb-doped material (A1) is, within experimental error of the measurements, unaffected by exposure to water at pH 6: the undoped material B in contrast shows the same marked Ba-depleted zone at pH 6 as pH 3. There is thus no doubt that $BaTiO_3$, in common with other perovskites,[18] tends to release its A site (alkaline earth) cations into an aqueous medium. Under hydrothermal conditions, the depleted layer found was deeper.[14] The reason for the differences in behaviour between the two types of material is not immediately obvious, but seems likely to be related to the ($\sim$0·5%) Nb-dopant in material A1. The Nb_2O_5 is incorporated into $BaTiO_3$ powders as a grain-growth inhibitor.[38,39] At the grain boundaries, replacement of Ba^{2+} by Nb^{5+} results in the formation of barium ion vacancies:[40]

$$Nb_2O_5 = 2Nb_{Ba}^{3+} + 5O_O + V_{ba}^{2-} \quad (5)$$

If Ba^{2+} is released preferentially from the grain boundaries (as might be expected), then a higher V_{Ba}^{2-} concentration in the boundaries might tend to operate against the release mechanism by lowering the Ba^{2+} activity gradient. More work is needed on polycrystalline $BaTiO_3$ of different grain sizes to establish the bases for these differences.

The reason for the solubility of the sintered $BaTiO_3$ materials, as evidenced by the Ba^{2+} depth profile, and the absence of any changes in surface stoichiometry for the $BaTiO_3$ powders, is ascribed to the high (200–800 mg dm^{-3}) background Ba^{2+} concentration provided by the dissolving, and more readily soluble $BaCO_3$. The solubility of the $BaTiO_3$ phase through the reaction (1) is likely to be suppressed.

It is also possible that the mechanism of hydrolysis of $BaTiO_3$ sintered disks is initiated by the hydrolysis of the $BaCO_3$ layer present, releasing the activation energy necessary for hydrolysis of $BaTiO_3$. This mechanism would not be available to $\sim 1\,\mu$m powders, because such a $BaCO_3$ layer was not identified at their surface.

5 Conclusions

$BaTiO_3$ aqueous suspensions released significant concentration of barium ions, the concentration of which increases as pH decreases. There was no change in particle morphology that was detectable by SEM neither was there any change at the surface detected by TEM, a part from the crystallisation of $BaCl_2$ on the dried particles surface previously treated at pH 4 (using HCl).

From the surface analysis on the particles by XPS, there was no evidence for dissolution of the powders, or for any different behaviour between Nd-doped and undoped powders. However, a 20 nm layer depleted in Ba with respect to the nominal stoichiometry was found on sintered material after exposure to water. This effect is not important with powders probably because of suppression of the hydrolysis by the high concentration of Ba^{2+} released from carbonate contamination. The extent of the hydrolysis seen appears to be lower with the Nb-doped material. A similar 20 nm layer slightly depleted in Ba^{2+} could only be observed after 12 h exposure to pH 3. This different behaviour as compared with the undoped material might depend on grain boundary related phenomena, such as the depletion of Ba^{2+} ions at the grain boundaries. From the point of view of developing aqueous systems for tape-casting, it is important to note that the main source of Ba^{2+} ions in the aqueous suspension is the dissolution of $BaCO_3$ impurity present and not the dissolution of $BaTiO_3$. Since the surface analysis showed that the two powders studied have very similar surfaces, it is expected that the subsequent behaviour of their colloidal dispersions will not be influenced by their nature (doped or undoped) or their preparation route.

Acknowledgements

This work has been supported by the Commission of the European Communities 'Human Capital and Mobility' Fellowship ERBCHBICT 941697. Powders A1, A2 and C were supplied by Becks Electronics, UK. The authors wish to thank Dr. l. Bertóti and Dr. J. Szépvölgyi (Research Laboratory for Inorganic Chemistry, Hungarian Academy of Sciences, H-1112 Budapest, Budaörsi út 45, Hungary) who carried out a number of XPS analyses.

References

1. Moreno, R., The role of slip additives in tape-casting technology, Part I: solvents and dispersants. *Am. Ceram. Soc. Bull.*, 1992, **71**(10), 1521–1531.
2. Jaffe, B., Cook, W. R. and Jaffe, H., In *Piezolectric Ceramics*. Academic Press, London, 1971, pp. 50.
3. Kinoshita, K. and Yamaji, A., Grain size effects on dielectric properties in $BaTiO_3$. *J. Appl. Phys.*, 1976, **47**(1), 371–373.
4. Nièpce, J. C., Some aspects of the influence of particle size on properties and behaviour of a dielectric materia: example of barium titanate. In *Surfaces and Interfaces of Ceramic Materials*, Vol. 73, ed. L. C. Dufour, C. Monty and G. Petot-Ervas. NATO Series, Series E: Applied Sciences 1989, pp. 521–533.
5. Anderson, D. A., Adair, J. H., Miller, D., Biggers, J. V. and Shrout, T. R., Surface chemistry effects on ceramic processing of $BaTiO_3$ powder. In *Ceramic Transactions 1. Ceramic Powder Science II*, ed. G. L. Messing, R. R. Fuller and H. A. Housner. American Ceramic Society, Ohio, 1998, pp. 485–492.
6. Miller, D. V., Adair, J. H., and Newnham, R. E., Dissolution of barium from barium titanate in non-aqueous solvents. In *Ceramic Transactions 1. Ceramic Powder Science II*, ed. G. L. Messing, R. R. Fuller and H. A. Housner. American Ceramic Society, Ohio, 1988, pp. 493–500.
7. Nesbitt, H. W., Bancroft, G. M., Fyfe, W. S., Karkhanis, S. N., Nishijima, A. and Shin, S., Thermodynamic stability and kinetics of perovskite dissolution. *Nature*, 1981, **289**, 258–262.
8. Myhra, S., Savage, D., Atkinson, A. and Riviere, J. C., Surface modification of some titanate minerals subjected to hydrothermal chemical attack. *Am. Mineralogist*, 1984, **19**, 145–160.
9. Lencka, M. M. and Riman, R. E., Thermodynamic modelling of hydrothermal synthesis of ceramic powders. *Chem. Mat.*, 1993, **5**, 61–70.
10. Lencka, M. M. and Riman, R. E., Hydrothermal synthesis of perovskite materials; thermodynamic modelling

and experimental verification. *Ferroelectrics*, 1994, **151**, 159–164.
11. Slamovich, E. B. and Aksay, I. A., Structure evolution in hydrothermally processed (< 100°C) $BaTiO_3$ films. *J. Am. Ceram. Soc.*, 1996, **79**(1), 239–247.
12. Osseo-Asare, K., Arrigada, F. J. and Adair, J. H., Solubility relationships in the coprecipitation synthesis of barium titanate heterogeneous equilibria in the Ba–Ti–C_2O_4–H_2O system. In *Ceramic Transactions 1. Ceramic Powder Science II*, ed. G. L. Messing, R. R. Fuller and H. A. Housner. American Ceramic Society. Ohio, 1988, pp. 47–53.
13. Bendale, P. S., Venigalla, J. R., Ambrose, E. D., Verink, J. R. and Adair, J. H., Preparation of barium titanate films at 55°C by an electrochemical method. *J. Am. Ceram. Soc.*, 1993, **76**(10), 2619–2627.
14. Myhra, S., Smart, R. St. C. and Turner, P. S., The surfaces of titanate minerals, ceramics and silicate glasses: surface analytical and electron microscope studies. *Scanning Microscopy*, 1988, **2**, 715–734.
15. Blanco López, M. C., Fourlaris, G., Rand, B. and Riley, F., Characterisation of barium titanate powders Part I: barium carbonate identification. *J. Am. Ceram. Soc.*, in press.
16. Myhra, S., Atkinson, A., Riviere, J. C. and Savage, D., Surface analytical study of Synroc subjected to hydrothermal attack. *J. Am. Ceram. Soc.*, 1984, **67**(3), 223–227.
17. Kastrissos, T., Stephenson, M., Turner, P. S. and White, T. J., Hydrothermal dissolution of perovskite: implications for synroc formulations. *J. Am. Ceram. Soc.*, 1987, **10**(7), C144.
18. Turner, P. S., Jones, C. F., Myhra, S., Neall, F. B., Pharm, D. K. and Smart, R. St. C., Dissolution mechanism of oxides and titanate ceramics. Electron microscope and surface analytical studies. In *Surfaces and Interfaces of Ceramic Materials* Vol. 173, ed. L. C. Dufour, C. Monty and G. Petot-Ervas. NATO Series, Series E: Applied Sciences 1989, pp. 663–690.
19. Myhra, S., Bishop, H. E. and Rivière, J. C., Surface analysis features of Sybroc B and C. *Surface Technology*, 1983, **19**, 145–160.
20. Myhra, S., Bishop, H. E. and Rivière, J. C., Investigation by X-ray phtoelectron spectroscopy of surface features of some titanate materials. *Surface Technol.*, 1983, **19**, 161–172.
21. Briggs, D. and Seah, M. P., *Practical Surface Analysis, Volume I: Auger and X-ray Photoelectron Spectroscopy*. Second edition, John Wiley & Sons, Chichester, UK, 1990.
22. Moulder, J. F., Stcke, W. F., Sobol, P. E., and Bomben, K. D., *Handbook of X-ray Photoelectron Spectroscopy* ed. J. Chastain, R. C. King. Physical Electronics Inc., Eden Prairie, Minnesota 55344 USA, 1995.
23. Blanco López, M. C., Rand, B., and Riley, F. L., The properties of aqueous of aqueous phase suspensions of barium titanate. *J. Eur. Ceram. Soc.*, 1997, **17**, 281–287.
24. Sullivan, J. L., Saied, S. O. and Bertóti, I., Effect of ion and neutral sputtering on single crystal TiO_2. *Vacuum*, 1991, **42**, 1208.
25. Bertóti, I., Kelly, R., Mohai, M. and Toth, A., A possible solution to the problem of compositional change with ion bombardment oxides. *Surf. Interf. Anal.*, 1992, **19**, 291–297.
26. Bertóti, I., Kelly, R., Mohai, M. and Toth, A., Response of oxides to ion bombardment: the difference between chemically inert and reactive ions. *Nucl. Instrum. Methods*, 1993, **B80/81**, 1219–1225.
27. Hung, C. C., Riman, R. E. and Caraciolo, R., An XPS investigation f commercial barium titanate powders. In *Ceramic Transactions, Vol. 12, Ceramic Powder Science III*, ed. G. L. Messing, S. Hirano and H. Housner. The American Ceramic Society Inc. Westerville, 1990, pp. 17–25.
28. Hérard, C. A., Faivre, A. and Lemaître, J., Surface decontamination treatments of undoped $BaTiO_3$ Part I: powders and green body properties. *J. Eur. Ceram. Soc.*, 1995, **15**, 145–153.
29. Weast, R. C., *Handbook of Chemistry and Physics*, 64th edn. CRC Press, Florida, pB-72.
30. Cabrera, A. L., Vargas, F. and Zarate, R. A., Adsorption of carbon dioxide by barium titanate: evidence of absorption process mediated by a dipole-dipole interaction. *J. Phys. Chem. Solids*, 1994, **55**, 1303–1307.
31. Tascón, J. M. D. and Tejuca, L. G., Adsorption of CO_2 on the perovskite-type oxide $LaCO_3$. *J. Chem. Soc. Faraday Trans. 1*, 1981, **77**, 591–602.
32. González-Tejuca, L., Rochester, C. H., García Fierro, J. L. and Tascón, J. M. D., Infrared spectroscopic study of the adsorption of pyridine, carbon monoxide and carbon dioxide on the perovskite-type oxides $LaMO_3$. *J. Chem. Soc. Faraday Trans. 1*, 1984, **80**, 1089–1099.
33. Proust, C., Husson, E. and Erre, R., XPS measurements on $BaTiO_3$ ceramics elaborated by a chemical route. *Electroceramics V, International Conference on Electronic Ceramics and Applications*, 2-4 September 1996, ed. J. L. Baptista, J. A. Labrincha, P. M. Vilarinho, University of Aveiro, Aveiro, Portugal, pp. 256–260.
34. Yamada, Y. and Chiang, Y. M., Nature of cation vacancies formed to compensate donors during oxidation of barium titanate. *J. Am. Ceram. Soc.*, 1995, **78**(4), 909–914.
35. González-Elipe, A. R., Sans, J. M., Fernández, A., Espinós, Munuera, G., Chemical changes in titanate surface induced by Ar+ ion bombardment. *Proc. ECASIA '91*, Wiley & Sons, Chichester, 1992.
36. Leinen, D., Fernandez, A., Espinós, J. P. and González-Elipe, A. R., Influences of the energy on the chemical effects induced in oxides during bombardment with Ar^+ nad O_2^+. *Proc. ECASIA '91*, Wiley & Sons, Chichester, 1996.
37. Desu, S. B. and Payne, D. A., Interfacial segregation in perovskites: II, Experimental evidence. *J. Am. Ceram. Soc.*, 1990, **73**(1), 3398–3406.
38. Wilson, J. M., Barium titanate. *Am. Ceram. Soc. Bull.*, 1995, **74**, 106–110.
39. Xue, L. A., Additives and the control of grain growth in barium titanate ceramics. PhD thesis, University of Leeds, 1987.
40. Chiang, Y. M. and Takagi, T., Grain boundary chemistry of barium titanate and strontium titanate: I, high-temperature equilibrium space charge. *J. Am. Ceram. Soc.*, 1990, **73**(11), 3279–3285..